

NJC

Accepted Manuscript



This is an *Accepted Manuscript*, which has been through the Royal Society of Chemistry peer review process and has been accepted for publication.

Accepted Manuscripts are published online shortly after acceptance, before technical editing, formatting and proof reading. Using this free service, authors can make their results available to the community, in citable form, before we publish the edited article. We will replace this *Accepted Manuscript* with the edited and formatted *Advance Article* as soon as it is available.

You can find more information about *Accepted Manuscripts* in the [Information for Authors](#).

Please note that technical editing may introduce minor changes to the text and/or graphics, which may alter content. The journal's standard [Terms & Conditions](#) and the [Ethical guidelines](#) still apply. In no event shall the Royal Society of Chemistry be held responsible for any errors or omissions in this *Accepted Manuscript* or any consequences arising from the use of any information it contains.



Journal Name

ARTICLE

Exploring High k Dielectric Behavior of Bio-Carbon Reinforced Cyanate Ester Nanocomposites

Pichaimani Prabunathan^a, Krishnan Srinivasan^b, Arumugam Hariharan^b, and Muthukaruppan Alagar*^a

Received 00th January 20xx,
Accepted 00th January 20xx

DOI: 10.1039/x0xx00000x

www.rsc.org/

In the present work, the surface of the bio-carbon (AC) derived from rice husk has been functionalized with 3-aminopropylsilane. The functionalized bio-carbon (FAC) was then used as reinforcement for cyanate ester (CE) matrix to obtain FAC/CE bio-composites. The morphology, thermal, electrical conductivity, and dielectric properties of FAC/CE bio-composites were studied with respect to the FAC loading. It was found that the introduction of the FAC reduces the heat-release rate and increases the degradation temperature, consequently the char residue of cyanate ester matrix increases. The glass-transition temperature (T_g) obtained infers that the introduction of FAC increases the T_g of the resulted nanocomposites through restricting the mobility of the CE matrix. Moreover, FAC reinforcement improves the overall conductivity and act as capacitors in the resulted nanocomposites. Finally, due to its higher capacitive behavior the over all dielectric constant of the developed FAC/CE nanocomposites get significantly increased and show highest value of dielectric constant (k = 8.13) for 4 wt % FAC/CE nanocomposite. The results from thermal and dielectric studies infers that the bio-carbon reinforced CE nanocomposites can be used as embedded capacitors into the inter layers of printed circuit boards (PCBs) and as electromagnetic interference shielding/antistatic material.

Introduction

Polymer carbon composites with high dielectric constant are well-known for anti-static coatings, electromagnetic interference shielding, embedded capacitors and gas sensors applications¹⁻⁵. The dielectric properties and conductivity of different types of industrial polymer composites have been described and reported⁶⁻¹⁰. However, the reported polymer composite involves less economical, hard synthetic carbon sources such as carbon nanotubes, graphenes and ceramic reinforcements¹¹⁻¹⁵. Recently, demand over fossil fuels, awareness about environment creates interest particularly in developing materials from renewable, recyclable, sustainable, and biodegradables¹⁶⁻²⁰. Mainly, polymer composites materials derived from renewable resources, biomass and recyclable wastes find suitable industrial and engineering applications²¹⁻²⁴. However, no significant attention has been paved about the bio-reinforcements as like bio-polymers, which also possess equivalent contribution to enhance the properties of polymers.

Graphene and carbon nanotubes (CNTs) are the commonly used carbon reinforcement because of superior properties such as large surface area, great flexibility and good mechanical properties. However, these carbon sources still exhibit unsatisfactory behaviour mainly insuperable restacking or aggregation²⁵⁻²⁸. In addition, due to their restricted dimensions and presence of excess oxygen functionality on the surface of graphene/graphite oxide critically affects the conductivity path and favours the resistivity. Moreover, unaffordable price and tedious synthetic routes are also chief reasons that hinder the practical utilization of graphene, CNT towards commercialization. So, synthesis of facile and low-cost carbon materials with desirable properties has become an advanced research²⁹⁻³². In this view, carbon derived from bio-source attracted great attention of researcher. Bio-carbon obtained from various bio-mass sources also possesses Sp² hybridized carbon skeleton and graphitic structures upon high temperature carbonization. Moreover they exhibit excellent physicochemical properties such as high surface area, porosity, conductivity and

^aPolymer Composite Lab, Department of Chemical Engineering, Anna University, Chennai, 600 025, Tamilnadu, India.

^bDepartment of Chemistry, Anna University, Chennai 600 025, Tamilnadu, India.

*E-mail : mkalagar@yahoo.com muthukaruppanalagar@gmail.com

Fax: +91 4422359164; Tel: +91 4422359164.

interconnectivity of particles and find wide range of engineering applications. Bio-carbons are majorly pyrolyzed product of cellulose and lignin rich biomass at low cost than other carbon products. Bio-carbon is likely possessing amorphous carbon structures and upon treating beyond 700 °C, forms a conductive phase. It is also found that the non-graphitic structures of bio-carbon can be tuned with suitable functional groups in order to form more chemical bonds with a polymer matrix. However, the research on using bio-carbon reinforced polymeric materials is very limited, in particular electrical properties.

Rice husk is well known biomass for its rich cellulose and lignin content. It possesses various constituents such as 22% lignin, 38% cellulose, 18% hemicelluloses, 20% ash and 2% extracts, which differs accordingly with growing conditions³³⁻³⁶. In recent decades, using rice husk ash and silica based polymer bio-composites were reported³⁷⁻⁴⁰. In our previous work, we reported the low *k* dielectric behaviour of mesoporous silica derived from rice husk reinforced epoxy bio-composite⁴¹. However, polymer bio-composites from activated carbon of rice husk with industrial value resins are not significant accounted. In this view, bio-carbon of rice husk reinforced polymer composite may results materials with high dielectric constant with improved conductivity and offers wide scope for industrial engineering applications.

Recently, cyanate ester (CE) resin became superior to other industrial valuable thermoset resins. For example, it possesses good mechanical properties at elevated temperature than epoxy resins and comparatively low moisture absorption with less toxicity than bismaleimide (BMI) resins⁴¹⁻⁴⁵. Consequently, CE emerged as a promising thermoset matrix in structural aerospace engineering, electronic device fabrications, as microwave-transparent composites, and as adhesives⁴⁶⁻⁴⁸. However, due to its low dielectric constant ($k = 2.8-3.2$) behaviour, its usage for high *k* dielectric applications are limited.

In the view and with our continuing interest to develop bio-composites, an attempt has been made to develop high *k* cyanate ester bio-composite using surface functionalized activated carbon derived from biomass rice husk. Here, activated carbon obtained from rice husk has been surface modified with 3-aminopropylsilane and reinforced with cyanate ester matrix via thermal curing. Particularly, dielectric constant, conductivity and resistivity of the developed bio-composites were studied and discussed in detail, which may offer wide scope in modern composites technology advancement. In addition, their thermal and morphological behavior are also studied and discussed. These may provide a new platform in the design of printed circuit board materials.

Experimental

Materials

Cyanogen bromide, acetone, bisphenol-A, triethyl amine (TEA), NaOH were obtained from Merck, India. 3-aminopropyltriethoxysilane (APS) was purchased from Sigma Aldrich, India. The rice husk was collected from the local sources of Tamilnadu, India.

Synthesis of Cyanate Ester (CE) 2,2-bis(4-cyanatophenyl)propane

A three-necked round-bottomed flask, equipped with a magnetic stirrer, a dropping funnel, and a drying tube, was charged with bisphenol-A (10 g, 0.0289 mol) and cyanogen bromide (6.7 g, 0.0635 mol). The reactants were dissolved in acetone (75 ml), and the solution was cooled to below -5 °C in a salt ice bath. Triethylamine (7.3 g, 0.0722 mol) was added in dropwise via the dropping funnel to the reaction mixture. After the addition of triethylamine, the reaction mixture was stirred for 1 h at -5°C and 1 h at room temperature. The precipitate was washed with water to remove the excess triethylamine and hydrobromide (as a by-product) and filtered. A white solid obtained was crystallized using 50/50 ethanol/water mixture to yield 7.2 g (63%) of product (Scheme 1).

Synthesis of Activated Carbon (AC) from Rice Husk

Activated carbon (AC) was prepared from rice husk as per the reported procedure⁴⁹. First, the rice husk was washed with water to remove the dirt and other contaminants, dried at 110 °C for 12 h and then the rice husk was carbonized at 400 °C under nitrogen atmosphere for 90 min in a tubular furnace. Second, the carbonized sample was digested with strong alkali NaOH with a weight ratio of (1:3) dried at 120 °C for 12 h. Then, carbonization was carried out at 400 °C for 30 min and at temperature 800 °C for 60 min to obtain activated carbon. Then, the carbonized product was grounded, neutralized by 0.1 M HCl solution and washed several times with hot distilled water till the pH becomes

neutral (7.0). The resulted activated carbon sample was dried under vacuum at 120 °C for 24 h and then its surface was functionalized with APS.

Surface Functionalization of Activated Carbon (FAC)

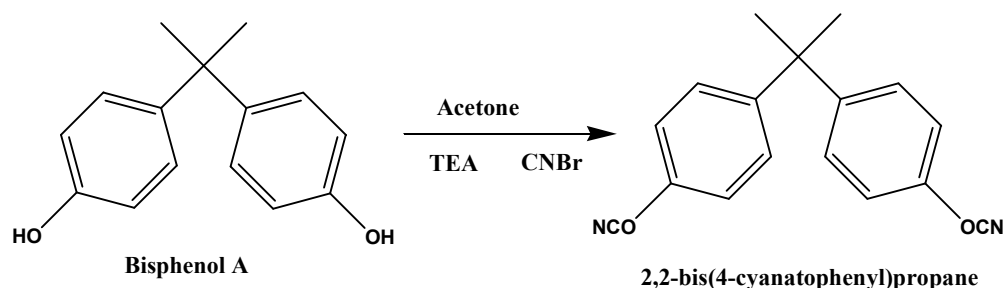
The surface of the activated carbon was initiated with functional group such as acid, hydroxyl, etc via, thermal treatment at 300 °C. Then, the sample was dispersed in ethanol under ultrasonic agitation for 30 min. Then APS was added and sonication was continued for another 30 min. The sonicated sample was further allowed to reflux for 24 h at constant stirring. Then the sample was centrifuged to collect the functionalized activated carbon (FAC) and washed several times using ethanol followed by hexane to remove the unreacted silane and dried in a vacuum oven at 60 °C for 24 h (Scheme 2).

Preparation of Functionalized Activated Carbon Reinforced Cyanate ester (FAC/CE) Nanocomposites

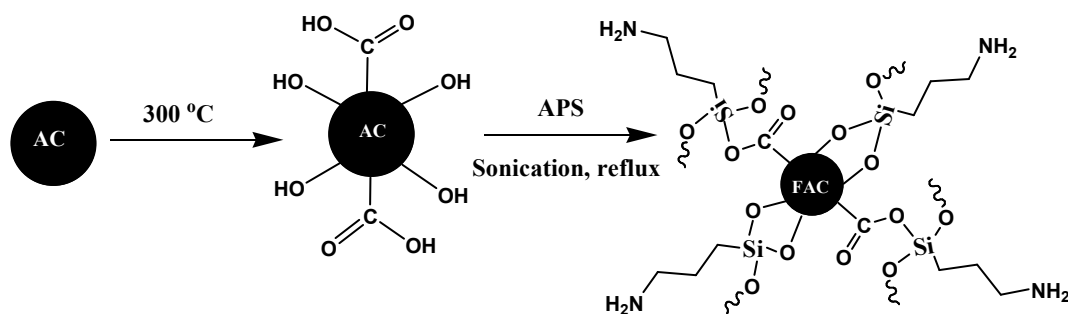
Various weight percent of FAC (1, 2, 3 and 4 wt %) were added separately to the 10 ml of 1,4 dioxane solution containing 2 g of cyanate ester (CE) monomer. The mixture was sonicated and allowed to stir for 24 h at room temperature. The resulted mixtures were then transferred into silane coated glass plates and allowed to evaporate for 6 h at room temperature. Further, the FAC/CE blend was subjected to thermal treatment in a stepwise manner at 100 °C, 150 °C, 200 °C and 250 °C for 1 h each (Scheme 3) to obtain FAC/CE nanocomposites. Further, the same procedure was adopted to obtain neat CE matrix by curing CE monomer without the addition of FAC.

Characterization

FT-IR spectra data were obtained from Perkin Elmer 6X FT-IR spectrometer. The solid state NMR spectra of AC and FAC were obtained from Bruker DRX-500 spectrometer, equipped with 4 mm MAS probes. Raman spectra were measured on a Lab RAM HR UV-VIS-NIR Raman Microscope from HORIBA JobinYvon (633 nm laser source). Nitrogen adsorption-desorption isotherms were measured at -196 °C on a Micromeritics ASAP 2010 volumetric adsorption analyzer. Prior to each adsorption measurement, the samples were evacuated at 100 °C, under vacuum ($p < 10\text{--}5$ mbar), in the degass port. The specific surface area of AC and FAC were determined from the linear part of the BET equation. The calorimetric analysis was performed on a Netzsch DSC-200 differential scanning calorimeter. Measurements were performed under a continuous flow of nitrogen (20 mL/min). About 10 mg of all samples were heated from ambient temperature to 350 °C and the thermograms were recorded at a heating rate of 10 °C/min under nitrogen atmosphere. Thermo gravimetric analysis (TGA) was performed on a Netzsch STA 409 thermo gravimetric analyzer calibrated with calcium oxalate and aluminium. About 50 mg of samples were heated from room temperature to 900 °C, under nitrogen atmosphere at a heating rate of 10 °C/min. A Hitachi S-4800 High resolution - Scanning Electron Microscope (HR-SEM) was used to record the morphologies of composites with their composition at 20 kV. HR-TEM images were captured using TECNAI G₂ S-Twin high resolution transmission electron microscope, with an acceleration voltage of 150 kV. TEM samples were prepared by dispersing the composites in ethanol and mounted on a carbon-coated Cu TEM grids and dried for 24 h at 30 °C to obtain a film of <100 nm in size. Dielectric constant, conductivity, dielectric loss values were obtained using Solartron impedance/gain phase analyzer 1260 at 30 °C in a frequency range of 1 MHz.



Scheme 1 Synthesis of cyanate ester monomer



Scheme 2 Functionalization of activated carbon with APS

Results and discussion

In order to study the dielectric and thermal properties of activated carbon from rice husk reinforced cyanate ester nanocomposites, the cyanate ester monomer and activated carbon were initially prepared. The synthesis of bisphenol-A based cyanate ester monomer was presented in the scheme 1. Further, the activated carbon from the rice husk was prepared using sodium hydroxide as activating agent. After, the surface functional group like hydroxyl, acid were initiated on the activated carbon via thermal treatment. Moreover, to promote better compatibility with organic polymer cyanate ester, the thermally treated activated carbon were subjected to surface modification using 3-aminopropylsilane as presented in scheme 2. Then, the prepared AC and FAC were subjected to various characterizations.

Spectral analysis of AC and FAC

It is well known that oxygen-containing functional groups are essential to modify the surface of the inorganic components with suitable silane agent. Thus, the prepared AC was subjected to thermal treatment. Further, the formation and presence of oxygen functionality were studied using FTIR and XPS analysis. Fig. 1a shows the FTIR spectra of AC and FAC. The three major peaks observed at 999, 3450 and 1690 cm^{-1} indicates and confirms the presence of hydroxyl and acid carbonyl groups⁵⁰. Moreover, the Fig. 1b shows the XPS survey scan of the thermally treated AC. The spectrum confirms the presence of C and O atoms through the 1s binding energy peak of both. Further, the deconvoluted XPS spectral of C 1s is shown in Fig. 1c. The spectrum shows strong binding energy peaks of C–C/C=C bonds at 284.7 eV, in addition to the several binding energy peaks of oxygen containing functional groups, such as C–OH at 286.1 eV, C=O at 287.9 eV, and O=C–OH at 289.3 eV. Hence it is evident that the surface of the AC was initiated with oxygen functionality^{51,52}.

Fig. 2 shows the Raman spectra of activated carbon (AC) and functionalized activated carbon (FAC) derived from bio-mass rice husk. Both AC and FAC show peaks at 1593 cm^{-1} and 1350 cm^{-1} which represent the G and D-bands and confirms the presence of Sp^2 hybridized as well as amorphous carbon respectively^{53,54}. It is interesting to note that both the AC and FAC spectra have the comparable vibration pattern with the similar intensity ratio of G-bands and D bands, I_G/I_D , as 1.04.

Further, the functionalization of activated carbon was strongly substantiated by the ^{13}C CPMAS NMR signals. Fig. 3a-b illustrates the ^{13}C spectra of AC and FAC. The signals appeared at 127.9 ppm (Fig. 3a) and 128.0 ppm (Fig. 3b) represents the presence of aromatic carbons of both AC and FAC respectively. In addition to the presence of aromatic carbon signals, the ^{13}C CPMAS spectrum of FAC presented in Fig. 3b shows new signals around 16-17 and 58-61 ppm. This up field signal corresponds to the presence of aliphatic carbons of APS and confirms the functionalization of FAC^{55,56}. Thus the new signals at 8.7, 22.9, 57.6, 67.0 and 71.9 ppm corresponds to the –Si–CH₂, –CH₃, Si–R–CH₂, –N–CH₂ and O–CH₂– carbon atoms respectively.

Addition to up field carbon signals, the ^{29}Si CPMAS NMR spectra of FAC also confirms the functionalization through the presence of Si signals. In Fig. 4a, ^{29}Si spectra of AC, no signal for the presence of silicon atoms was observed, whereas in Fig. 4b, the FAC two new signals were found at -57.1 and -65.8 ppm, which correspond to the T² and T³ silicon atoms

respectively^{55,56}. This result infers, the formation of new Si–O–C covalent bond linkages between the amine terminated silane and the –OH functionality of surface group of activated carbon through the condensation.

In addition to the NMR analysis, the binding energy spectra of FAC obtained from X-ray photoelectron confirms the functionalization of AC. The spectrum shows the presence of N and Si atoms respectively in addition to the C, and O atoms of FAC (Fig. 5a.). The binding energy signal of Si and N atom at 400, and 102 eV shown in Fig. 5b and 5c confirms the presence of APS and their grafting over the surface of the bio-carbon⁵⁷.

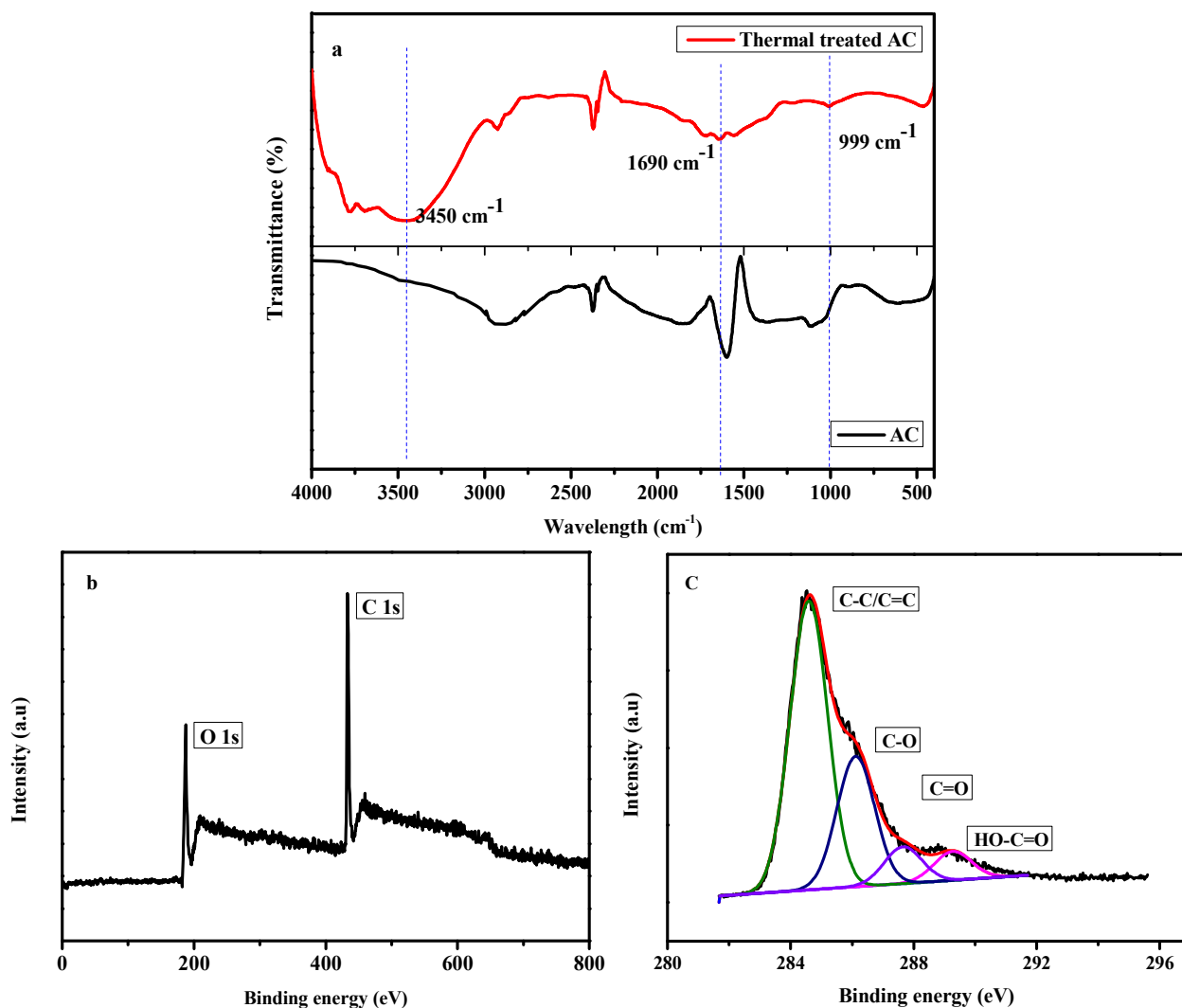


Fig 1a FTIR spectra, b) XPS survey of FA and FAC and c) XPS spectra of 1s C of FAC.

Journal Name

ARTICLE

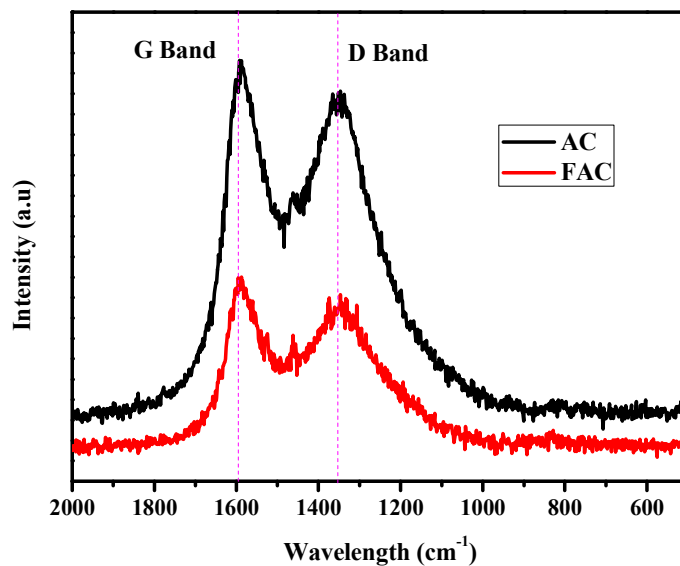
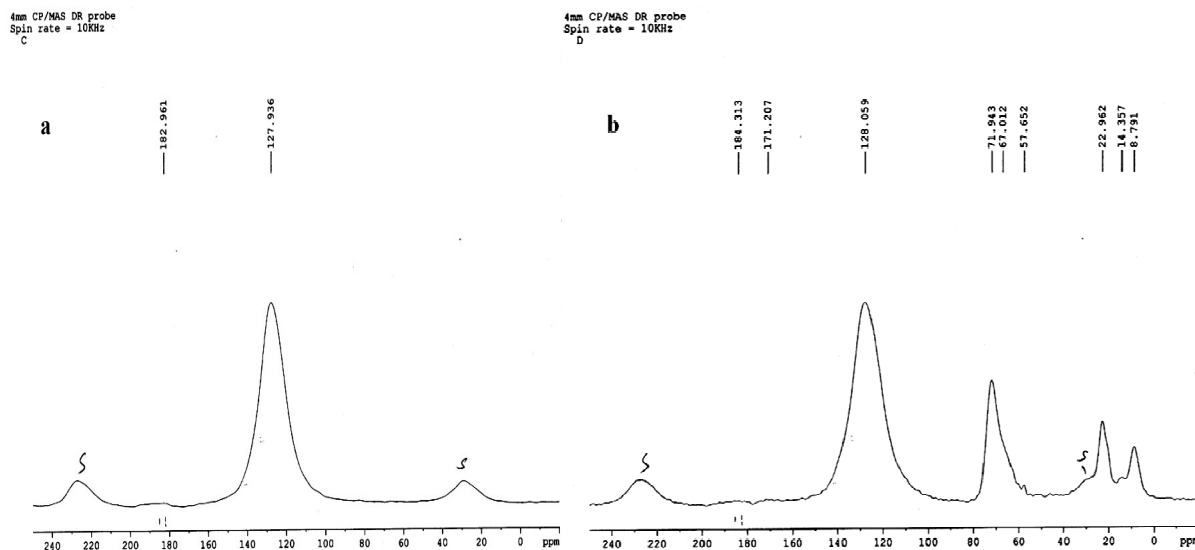


Fig.2 Raman spectra of AC and FAC

Fig.3 ^{13}C CP MAS NMR spectra of a) AC and b) FAC

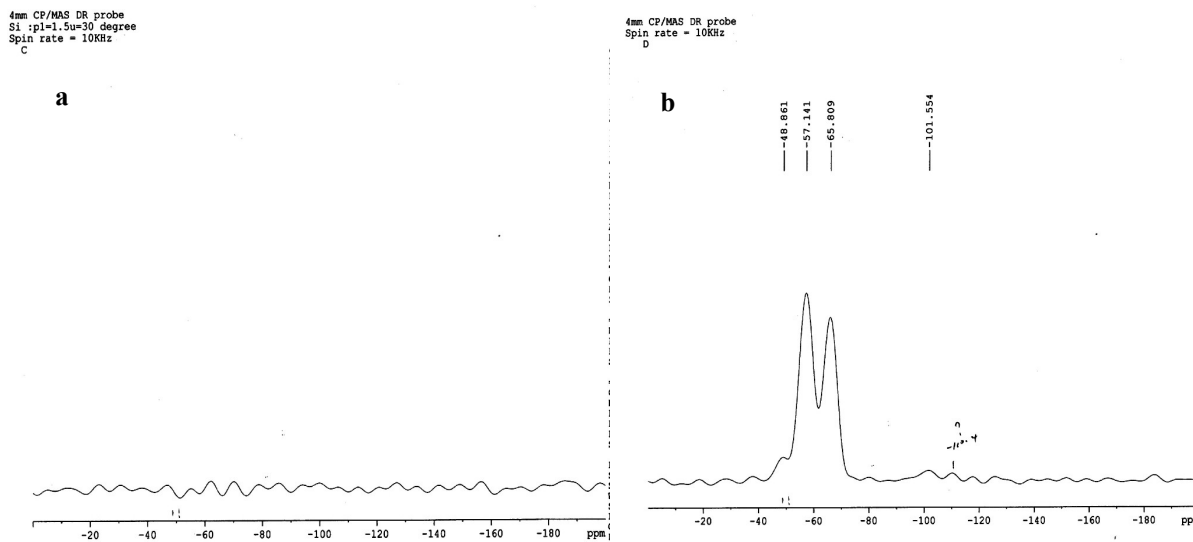


Fig. 4 ^{29}Si CP MAS NMR spectra of a) AC and b) FAC

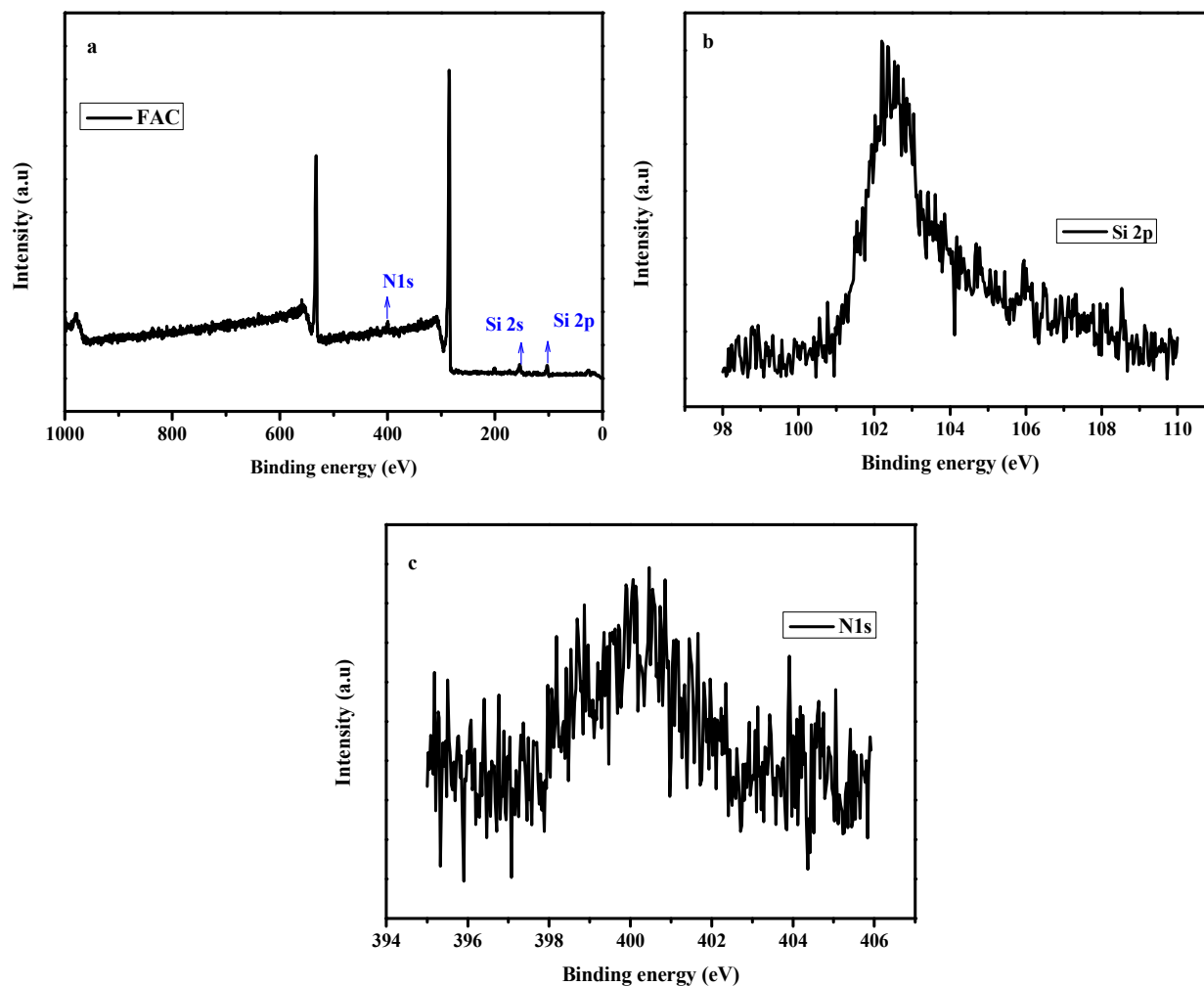


Fig. 5a) XPS Spectrum of FAC, b) binding energy curve of Si 2p and c) binding energy curve of N 1s

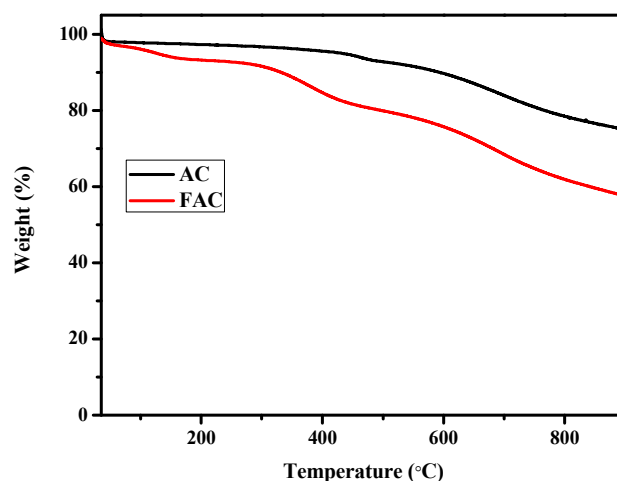
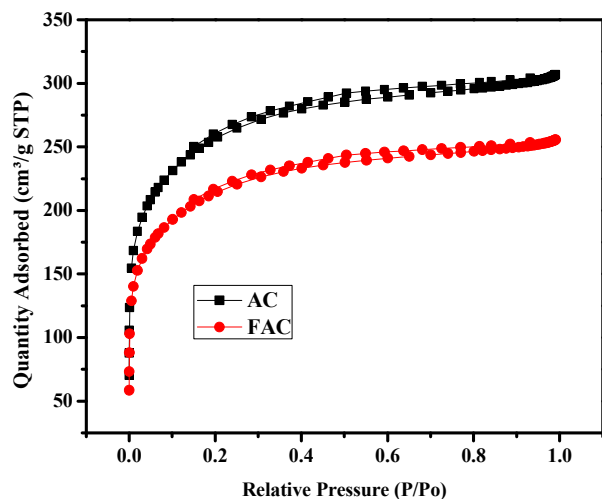


Fig. 6 Nitrogen adsorption-desorption isotherm of AC and **Fig. 7** TGA of AC and FAC

Textural and thermal analysis of AC and FAC

The textural properties of both AC and FAC were obtained from N₂ adsorption-desorption studies and the resulted isotherms were presented in Fig. 6. The isotherms of both AC and FAC exhibits type IV hysteresis loop and are in accordance with reported literature^{58,59}. It is noteworthy that the surface area of AC decreased after its surface functionalization. Thus the surface area of AC 894 m²/g decreased to 721 m²/g after functionalization also confirms the existence. The decrease in the surface area may due to the presence of APS on the surfaces^{60,61}. The high surface area of the bio-carbon provides strong interfacial interaction with the CE matrix through the surface functional groups. However, the surface functional groups present on FAC possess less thermally stability than that of AC and the corresponding thermo-gram was presented in Fig. 7. The less thermal stability of the FAC may be accounted for the presence of organic silane coupling agents, which began to degrade in two steps. The first step is associated with the removal of physically adsorbed water, whereas the second step involves the decomposition of the organic moiety, present on the integral part of the activated carbon. The thermo-grams of FAC shows 43 % weight loss, whereas that of the activated carbon (AC) shows only about 25 % weight loss at 900 °C. These results suggest that the higher weight loss of FAC occurred may due to the presence of silane moiety APS.

Characterization of FAC/CE nanocomposites

Spectral analysis

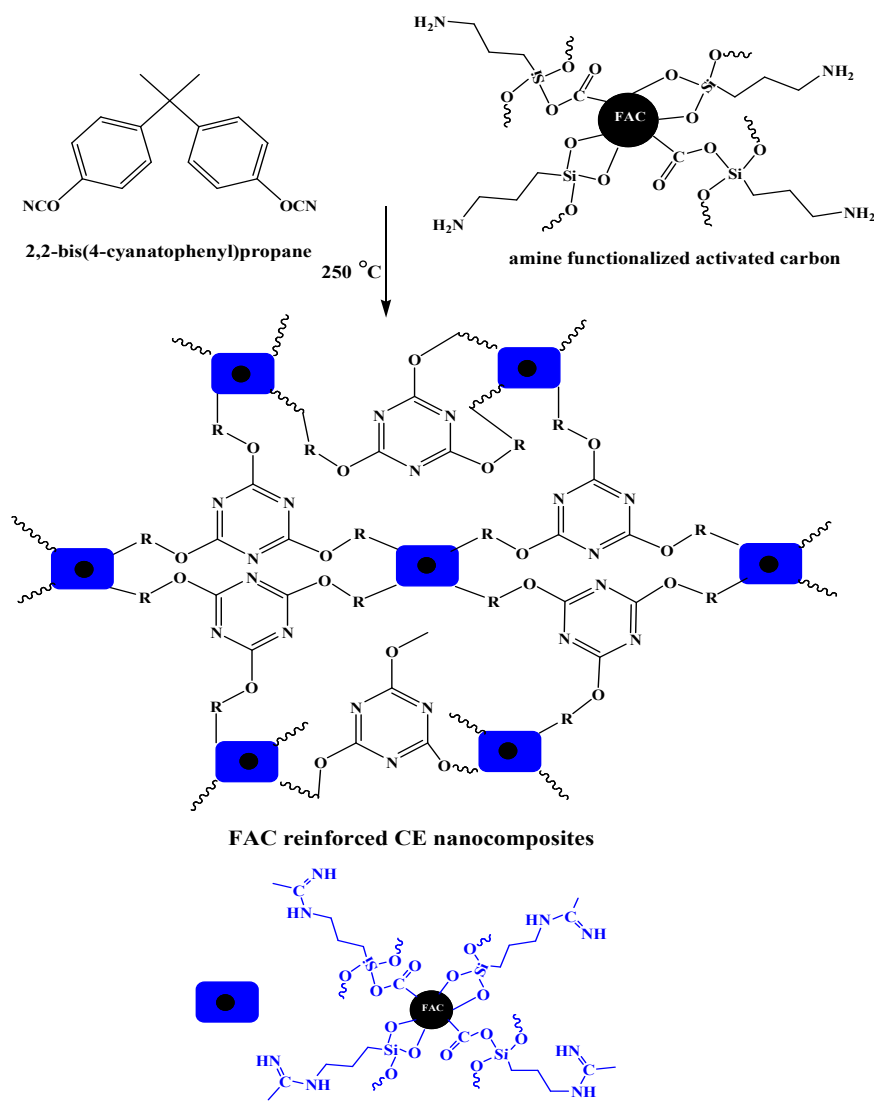
FAC reinforced cyanate ester bio-composites were prepared by incorporating 1, 2, 3 and 4 wt % of FAC into CE by thermal curing. The formation of FAC reinforced CE nanocomposites were illustrated in scheme 3. In order to ascertain the formation, the developed nanocomposites were analyzed with FTIR. The results obtained from FTIR analysis are shown in Fig. 8. The disappearance of peak at 2237 cm⁻¹ confirms the curing of cyanate ester group. However, the CE monomer exhibits the peak at 2237 cm⁻¹, which confirms the curing of CE monomers. Further, the appearance of peaks at 1365 and 1565 cm⁻¹ confirms the formation of triazine rings, which accounts for the polymerization of OCN group^{47,48}.

Thermal Properties

The weight loss at various temperatures of neat CE and FAC/CE bio-composites were studied by the thermo gravimetric and differential scanning analysis to ascertain their thermal stability and are presented in Fig. 9a-b and Table 1. Compared to the neat CE matrix, the FAC/CE bio-composites show a significant improvement in thermal stability and substantiate their permanency even at high temperature range. It can be seen that during pyrolysis under nitrogen the weight loss of neat CE matrix and FAC/CE bio-composites took place at a single step. However, upon addition of FAC, the thermal degradation rate gets slowed down. Thus, 4 wt % FAC/CE starts to degrade at 325 °C, whereas that of neat CE degrades at 274 °C. This

phenomenon can be attributed to the presence of well dispersed carbon reinforcement. The dispersed carbon act as a heat barrier and that hinder the transport of heat into the CE matrix. The simultaneous thermal curing of the cyanate ester resin along with FAC reinforcement forms a FAC intercalated organic inorganic hybrid network through bonding and thereby increases the interfacial interaction and compatibility between the CE matrix and FAC reinforcement. In addition to the interaction, interpenetration at a molecular level dispersion of FAC into the polymer matrix layer also acts as a contributing factor for the enhanced thermal stability⁶². Thus, the presence of FAC resists the breakup of the cyanurate rings of CE matrix. Due to these factors, the char yield of the composites increases as a function of carbon reinforcement. The final residual char weight (Table 1) of the composites increases as percentage weight of the FAC increase. Thus, the char yield of 4 wt % FAC/CE was about 13 % at 900 °C, whereas that of neat CE shows only 7% of char residue.

The Tg value of neat CE is found to be 234 °C, whereas upon addition of 4 % FAC into the CE matrix the Tg value shifted to 259 °C (Fig. 9b). This enhancement may be due to good interfacial interaction between the carbon reinforcement and cyanate ester in the nanocomposites. It is reported that in this interaction region between CE (polymer) layers surrounding the FAC interface, the conformational entropy and the chains kinetics of the polymeric material are significantly altered. Thus, the polymer chains in this region are under constrain and the movement of the polymeric chain segments gets retarded and restricted, which consequently shifts the Tg value of the resulted nanocomposites to higher temperature region^{62,63}.



Scheme 2 Schematic representation of formation of FAC/CE nanocomposites

Journal Name

ARTICLE

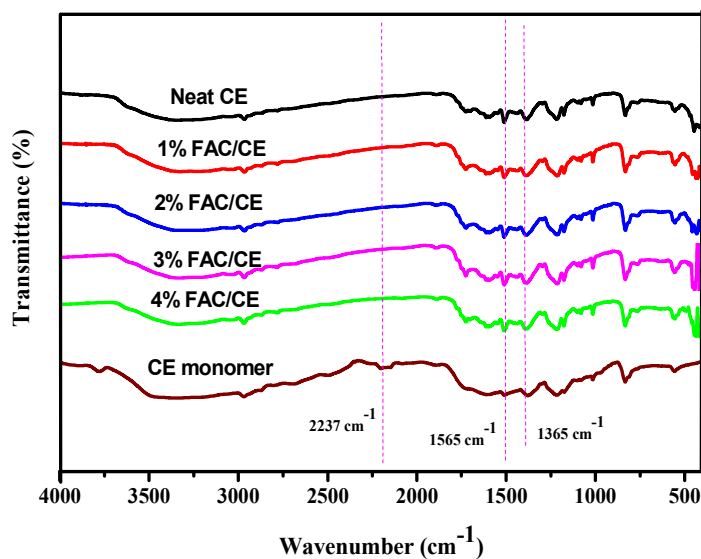


Fig. 8. FTIR spectra of CE monomer and FAC/CE nanocomposites

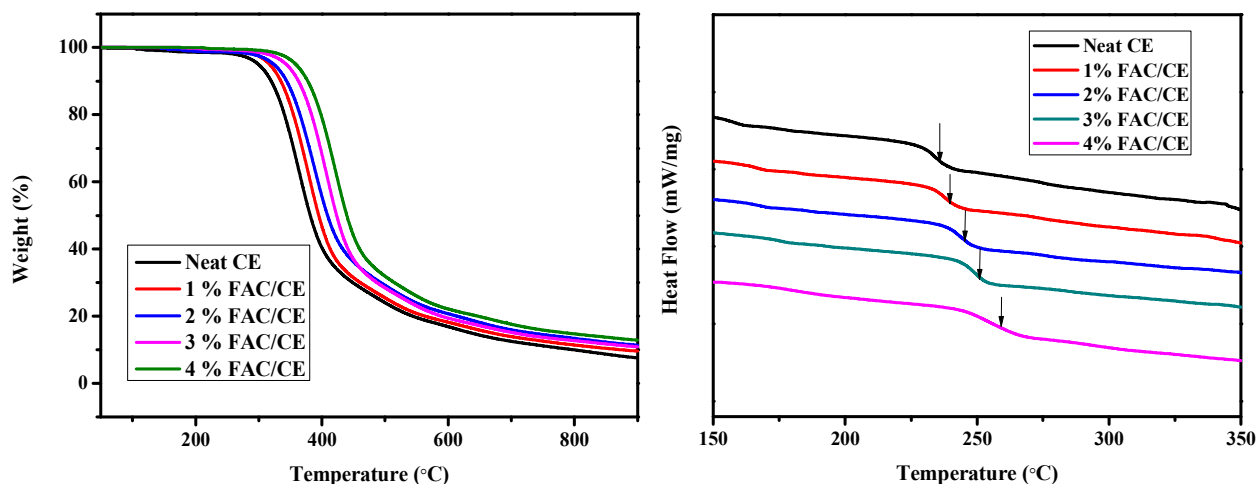


Fig. 9a-b TGA and DSC profile of neat CE and FAC/CE nanocomposites

Morphological Studies

The SEM images of the fractured surfaces of neat CE and FAC reinforced CE nanocomposites (FAC/CE) were shown in Fig. 10. Fig. 10 (a) of neat CE matrix shows the uniform fractured surface, which is very smooth and has no crack and discloses the characteristics of brittle fracture. However, the 3 and 4 wt % FAC/CE nanocomposites (Fig. 10.d-e), show a rough and irregular fractured surfaces. This confirms good compatibility resulted between the cyanate ester matrix and the FAC phase^{62, 64, 65}. The compatibility of the cyanate ester matrix with functionalized activated carbon confirms the formation of

passive layer through the chemical reaction occurred during curing between the amino groups of FAC with cyanate esters, which in turn forms insulating and passive layer over conductive FAC. Consequently, the formed layer, change the nature of surface polar groups in the resulted FAC/CE nanocomposites⁶⁶. Further, to ascertain the uniform distribution of FAC in the CE matrix HR-TEM analysis were performed and the images are presented in Fig. 11 (a) and (b). The TEM images of 2 wt % and 4 wt % FAC/CE nanocomposites show the uniform dispersion of bio-carbon in the CE matrix. The distribution of particles in the 4 wt % FAC/CE was found to be denser than that of 2 wt % FAC/CE. This in turn influences and contributes to the improvement of both electrical and thermal properties.

Chemical composition analysis

Moreover, the elemental composition of the neat CE, 2 wt % and 4 wt % FAC reinforced CE nanocomposites are shown in Fig. 12 and Table 2. The neat CE matrix shows 68.01 wt %, where as 2 and 4 wt % FAC reinforced CE nanocomposites show 69.84 % and 74.52 % carbon content. Further, with respect to the concentration of FAC the Si content in the composites also increases and reaches 2.45 % for 4 wt % FAC/CE nanocomposites.

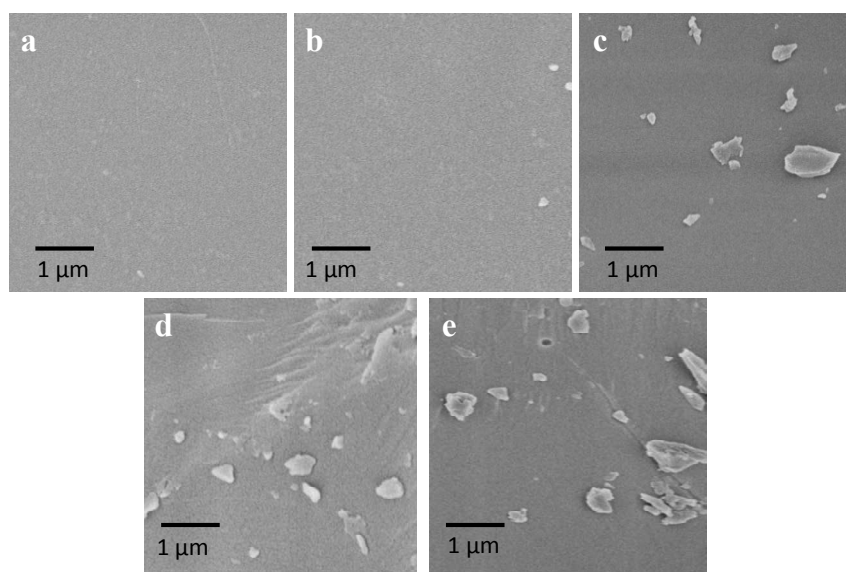


Fig. 10 SEM of a) neat CE, b) 1% c) 2% d) 3% and e) 4% FAC/CE nanocomposites

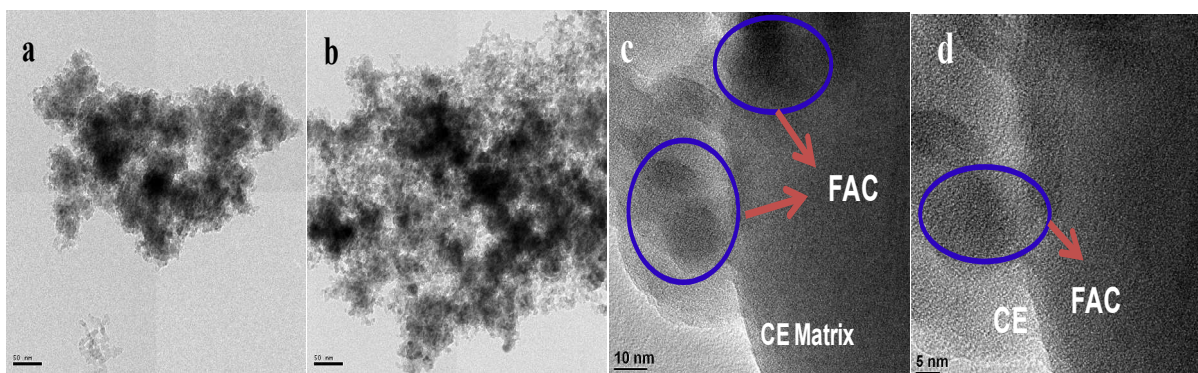


Fig. 11 HR-TEM of (a) 2%, (b) 4% FAC/CE nanocomposites at 50 nm, (c) and (d) 4% FAC/CE nanocomposites at 10 nm and 5 nm.

Conductivity Behaviour

The frequency dependency of AC conductivity at room temperature of the neat CE and FAC/CE bio-composites is presented in Fig. 12. The electrical conductivity of the neat CE matrix was observed as $7.63 \times 10^{-6} \text{ S} \cdot \mu\text{m}^{-1}$ at 1MHz, and that of the 1 wt% FAC reinforced CE bio-composites show an increased electrical conductivity as $1.68 \times 10^{-5} \text{ S} \cdot \mu\text{m}^{-1}$ at 1MHz. The conductivity of composites increase with increase in FAC content and reaches $1.44 \times 10^{-4} \text{ S} \cdot \mu\text{m}^{-1}$ at 1MHz when 4 wt % FAC was reinforced into CE bio-composites. It is worthy to note that the obtained AC conductivity value of the FAC/CE nanocomposites is found to be significantly comparable than the results available in literature using carbon black, graphite, MWCNT as reinforcement⁶⁷⁻⁷⁰. This phenomenon may be attributed due to the presence of the conductive carbon promotes the overall conductivity of the bio-composites. It is reported that carbonization above 600 °C affords high order conductivity. Thus reinforcing such carbon sources into polymeric material yield improved conductive behavior. Moreover, the surface functionalization also facilitates the dispersion of FAC in the CE matrix. When the content of FAC is low, the conductivity of the corresponding composites is also low. Because of the discontinuous distribution of FAC, the composites have lower conductivity with low wt % of FAC. Further, as shown in the TEM micrographs (Fig. 12) the distance between the FAC domains was reduced in 4 wt % FAC, when compared to 2 wt % FAC. Consequently, inter particle distance facilitated the movement of the charge from one carbon to another. The highly interactive strength and amplification of carbon reinforcement improves the conductivity of the resulted nanocomposites⁷¹⁻⁷³.

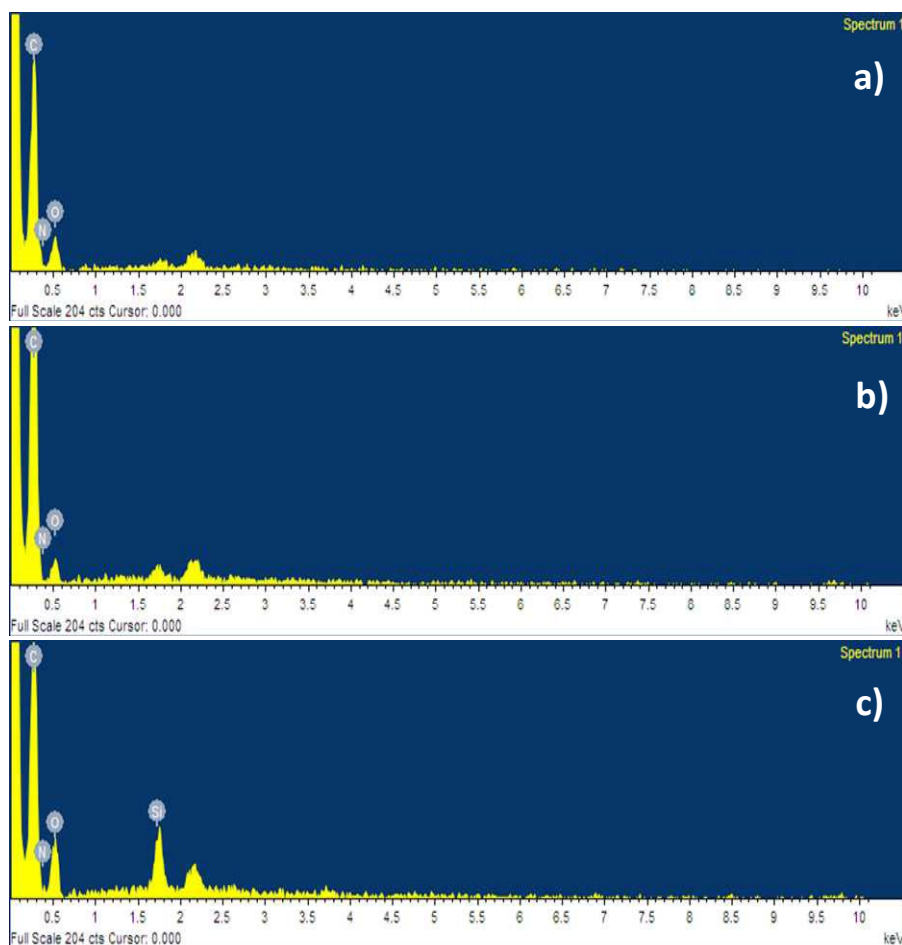


Fig.12 EDAX profiles of a) neat CE, 2 wt % and b) 4 wt % FAC/CE nanocomposites.

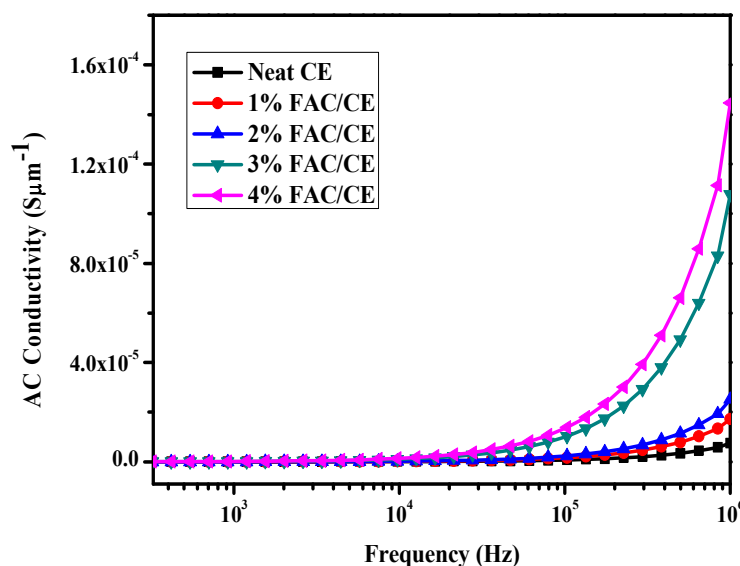


Fig. 13 AC conductivity profiles of neat CE matrix and FAC/CE nanocomposites

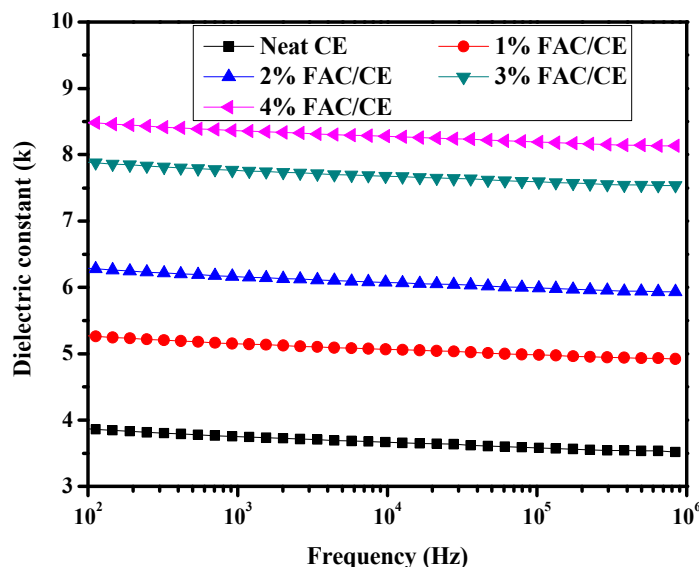


Fig. 14 Dielectric constant (k) profiles of neat CE matrix and FAC/CE nanocomposites

Dielectric properties

The dielectric properties of the FAC reinforced CE nanocomposites were studied by broadband dielectric spectroscopy from 1 Hz to 1 MHz at room temperature. The effect of reinforcing FAC into the CE matrix was well documented from the dielectric behavior of respective FAC/CE nanocomposites. Fig. 14 shows the frequency dependence of the dielectric constant and supports linear behavior over the whole frequency range for both CE matrix and FAC/CE nanocomposites. However, neat CE matrix possesses the lowest value of dielectric constant (3.5), whereas 4 wt % FAC/CE has the highest dielectric constant (8.1). Further, the value of dielectric constant obtained using bio-carbon of rice husk is comparably with those of commercial carbon black and CNT reinforcement^{10, 62, 74}. It is known that the dielectric properties polymer nanocomposites were mainly influenced by the dispersion of conductive reinforcement, surface area and the interface polarity. Here, due to the high surface area of FAC, the formation of the interface (the FAC–CE interface) appeared becomes more in the CE matrix. Thus, with increases in the FAC content, the FAC–CE interfaces are also increased. The increase in interfacial interaction promotes the dispersion of

the nano-sized bio-carbon throughout the matrix. The dispersed bio-carbon acts as mini capacitors, which in turn increases the overall dielectric constant of the FAC/CE composite materials. It is important to note that, even after the incorporation of the highly conductive carbon into the CE matrix, the dielectric value remains constant over the whole frequency region. This result indicates that the dielectric response is not dominated by the polarization of the space charges. The space charges on the interfaces of FAC were minimized due to the presence of APS. As a result, the accumulation of these nano-sized capacitors increases the overall capacitance of the composites and contributes to high dielectric value of FAC/CE composite materials⁷⁵⁻⁷⁷.

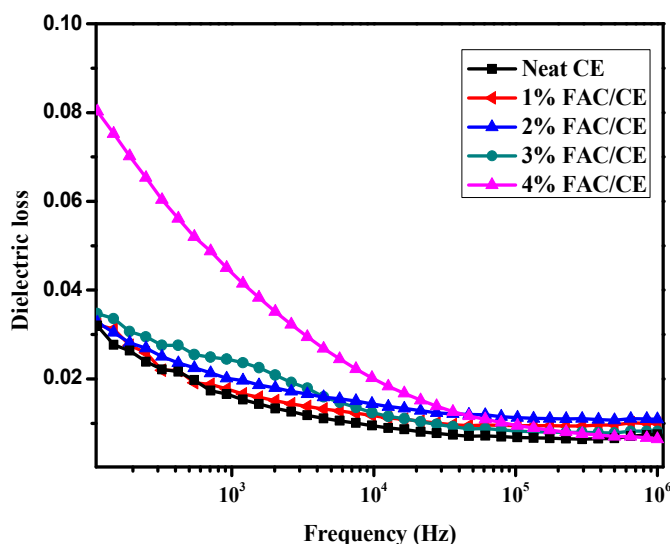


Fig. 15 Dielectric loss profiles of neat CE matrix and FAC/CE nanocomposites

Fig. 15 shows the plots of dielectric loss versus frequency for the neat CE and FAC/CE nanocomposites. At 1 MHz, the dielectric loss value for neat CE is about 0.006, whereas in the case of 1 wt% and 2 wt% of FAC reinforcement, the dielectric loss values are 0.009 and 0.011 at 1 MHz. Upon further loading of FAC i.e., 3 wt% and 4 wt% of FAC reinforcement the value of dielectric loss gets reduced to 0.008 and 0.007. However, the dielectric loss at lower frequency gets increased, which is due to conduction loss. In the case of conductive filler/polymer composites the loss of electric conduction and the loss of interfacial polarization causes over all dielectric loss phenomenon. The loss of electric conduction makes more contribution to dielectric loss than that of interfacial polarization, at relatively low frequency, so the dielectric loss of composites decreases with the increase of frequency. Therefore, for this type of composite the passivation of the conductive reinforcement is prerequisite⁷⁸⁻⁷⁹. However, in the present case it is inferred that the composites possess an obvious decrease in dielectric loss at higher frequency with the introduction of FAC. The obtained dielectric loss values are lower than the results of carbon sources such as CNT, carbon black^{10, 62, 74}. The decrease in the dielectric loss of the FAC/CE nanocomposites may be due to the following reasons, i) enhanced dispersion of the FAC forms a aligned direction rather than forming a conductive path and ii) the low order interfacial polarity of FAC. The presence of silica of APS on the surface of the bio-carbon provides not only improved interfacial interaction and also passivated the surface polar charges. The presence of silica in FAC and FAC/CE is evident from XPS and EDAX profile and discussed in earlier section. Thus, the bio based nanocomposites prepared in the present work with high dielectric value and low dielectric loss may have better dielectric applications.

Conclusions

The present work describes the development and characterization of high dielectric bio-composites obtained from renewable source rice husk based activated carbon reinforcement. Spectral evidences confirm the surface functionalization of activated carbon. Data resulted from electrical studies indicate that, the dielectric constant values are increased with increase in weight percentage of functionalized activated carbon into cyanate ester and the reverse trend in dielectric loss values are noticed. In addition, the increase in the weight percentage of reinforcement in cyanate ester matrix improves the values of Tg and also contributes to an improved thermal stability to the nanocomposites. From the micrograph, the homogeneous dispersion and efficient compatibility of bio-carbon with the cyanate ester matrix were confirmed. Data resulted from electrical and thermal studies inferred that these bio-

composite materials developed from renewable resource can be used as electromagnetic interference shielding/antistatic material and as embedded capacitors in printed circuit board with enhanced performance and improved longevity.

Acknowledgements

The authors thank BRNS, G. No: 2012/37C/9/BRNS, Mumbai, Govt. of India., for the financial support.

References

- 1 R.P. Ortiz, A. Facchetti, and T.J. Marks, *Chem. Rev.*, 2010, **110**, 205.
- 2 S.K. Bhattacharya and R.R. Tummala, *J. Mater. Sci. Mater. Electron.*, 2000, **11**, 253.
- 3 K.J. Albert, N.S. Lewis, C.L. Schauer, G.A. Sotzing, S.E. Stitzel, T.P. Vaid, D.R. Walt, *Chem. Rev.* 2000, **100**, 2595.
- 4 H. K. F. Cheng, N. G. Sahoo, Y. P. Tan, Y. Pan, H. Bao, L. Li, S.H.Chan, and J. Zhao. *ACS Appl. Mater. Interfaces* 2012, **4**, 2387.
- 5 M.C. Lonergan, E.J. Severin, B.J. Doleman, S.A. Beaver, R.H. Grubb, N.S. Lewis, *Chem. Mater.* 1996, **8**, 2298.
- 6 J.K.W. Sandler, J.E. Kirk, I.A. Kinloch, M.S.P. Shaffer¹, A.H. Windle. *Polymer*, 2003, **44**, 5893.
- 7 D. Ling, S. C. Jana. *Journal of Power Sources* 2007, **172**, 734.
- 8 M. Lahelin, M. Annala, A. Nykänen, J. Ruokolainen, J. Seppälä, *Composites Science and Technology* 2011, **71**, 900.
- 9 X. Liu, Y. Zhang, M. Zhu, X. Yang, C. Rong, and G. Wang. *Soft Materials*, 2011, **9**, 94.
- 10 M. Selvi, M. R. Vengatesan, P. Prabunathan, J. K. Song, and M. Alagar *Applied Physics Letters*, 2013, **103**, 152902.
- 11 L. Gu, G. Liang, Y. Shen, A. Gu, L. Yuan. *Composites: Part B*, 2014, **58**, 66.
- 12 J. Lu, K. S. Moon, J. Xu and C. P. Wong. *J. Mater. Chem.*, 2006, **16**, 1543.
- 13 B. M. Arbatti, X. Shan, and Z. Cheng. *Adv. Mater.* 2007, **19**, 1369.
- 14 T. Kuilla, S. Bhadra, D. Yao, N. H. Kim, S. Bose, J. H. Lee, 2010, **35**, 1350.
- 15 Z. Spitalsky, D. Tasis, K. Papagelis, C. Galiotis, *Progress in Polymer Science*, 2010, **35**, 357.
- 16 R. Wang, T. Schuman, R. R. Vuppapapati and K. Chandrashekhara, *Green Chem.*, 2014, **16**, 1871
- 17 J. J. Blaker, K. Y. Lee, X. Li, A. Menner and A. Bismarck, *Green Chem.*, 2009, **11**, 1321.
- 18 R. L. Quirino, T. F. Garrison and M. R. Kessler, *Green Chem.*, 2014, **16**, 1700.
- 19 M. S. Huda, L. T. Drzal, and M. Misra, *Ind. Eng. Chem. Res.* 2005, **44**, 5593.
- 20 T. A. Hassan, V. K. Rangari, and S. Jeelani, *ACS Sustainable Chem. Eng.* 2014, **2**, 706.
- 21 X. Zhu, Y. Liu, C. Zhou, S. Zhang, and J. Chen, *ACS Sustainable Chem. Eng.* 2014, **2**, 969.
- 22 R. Kuktaite, H. Türe, M. S. Hedenqvist, M. Gallstedt and T. S. Plivelic, *ACS Sustainable Chem. Eng.* 2014, **2**, 1439.
- 23 P. Prabunathan, K. Sethuraman and M. Alagar. *RSC Adv.*, 2014, **4**, 47726
- 24 M. M. Rahman, A. N. Netravali, B. J. Tiimob, and V. K. Rangari. *ACS Sustainable Chem. Eng.* 2014, **2**, 2329.
- 25 S. Liu, S. Sun and X. You. *Nanoscale* 2014, **6**, 2037.
- 26 G. Lota, G.; Fic, K.; Frackowiak, E. *Energy Environ. Sci.* 2011, **4**, 1592.
- 27 H.W. Wang, Z.A. Hu, Y.Q. Chang, Y.L. Chen, H.Y. Wu, Z.Y. Zhang, Y.Y. Yang. *J. Mater. Chem.* 2011, **21**, 10504.
- 28 M. F. El-Kady, V. Strong, S. Dubin, R.B. Kaner, *Science* 2012, **335**, 1326.
- 29 X.L. Wu, T. Wen, H.L. Guo, S. Yang, X. Wang, A.W. Xu. *ACS Nano* 2013, **7**, 3589.
- 30 D. Saha, Y. Li, Z. Bi, J. Chen, J.K. Keum, D.K. Hensley, H.A. Grappe, H.M. Meyer III, S. Dai, M.P. Paranthaman, *Langmuir* 2014, **30**, 900.
- 31 W. Chen, H. Zhang, Y. Huang, W. Wang. *J. Mater. Chem.* 2010, **20**, 4773.
- 32 W. Xiong, Y. Gao, X. Wu, X. Hu, D. Lan, Y. Chen, X. Pu, Y. Zeng, J. Su, and Z. Zhu. *ACS Appl. Mater. Interfaces* 2014, **6**, 19416.
- 33 M. Mahbubul Hassan, T. Takahashi, and K. Koyama, *Ind. Eng. Chem. Res.* 2013, **52**, 1275.
- 34 Y. Shen and K. Yoshikawa. *Ind. Eng. Chem. Res.* 2014, **53**, 10929.
- 35 A. Salanti, L. Zoia, M. Orlandi, F. Zanini, G. Elegir, J. Agric. *Food Chem.* 2010, **58**, 10049.
- 36 T.S. Galhardo, N. Simone, M. Goncalves, F.C.A. Figueiredo, D. Mandelli, and W.A. Carvalho. *ACS Sustainable Chem. Eng.* 2013, **1**, 1381.
- 37 M.Y. Ahmad Fuad, Z. Ismail, M.S. Mansor, Z. Mohd Ishak and A. K. Mohd Omar, *Polymer Journal*, 1995, **27**, 1002.
- 38 D. S. Chaudhary, M. C. Jollands, F Cser, *Silicon Chemistry*, 2002, **1**, 281.
- 39 K. Kanimozhi, P. Prabunathan, V. Selvaraj and M. Alagar. *RSC Adv.*, 2014, **4**, 18157.
- 40 H. S. Yang, H. J. Kim, H J Park, B J Lee, T S. Hwang. *Composite Structures*, 2006, **72**, 429.
- 41 P. Prabunathan, K. Sethuraman, M. Alagar, *High Performance Polymer*, 2014, **26**, 283.
- 42 I. Mondrago, L. Solar, A. Nohales, C.I. Vallo, C.M. Gomez, *Polymer*, 2006, **47**, 3401.
- 43 Y. Lin, J. Jin, M. Song, S.J. Shaw, C.A. Stone. *Polymer*, 2011, **52**, 1716.
- 44 C. Han, A. Gu, G. Liang, L. Yuan. *Composites: Part A*, 2010, **41**, 1321.
- 45 K.C James C. Seferis *Polymer Degradation and Stability*, 2001, **71**, 425.
- 46 K. Liang, G.L.H Toghiani, J.H. Koo, and C.U.Pittman, *J. Chem. Mater.* 2006, **18**, 301.
- 47 S. Devaraju, M.R. Vengatesan, M. Selvi, A. Ashok Kumar, I. Hamerton, J. S.Go, and M. Alagar. *RSC Advances*, 2013, **3**, 12915.
- 48 S. Devaraju, M.R. Vengatesan, M. Selvi, J.K.Song, and M. Alagar. *Microporous and Mesoporous Materials* 2013, **179**, 157.
- 49 K.L. Van, T. T. L. Thi, *Progress in Natural Science: Materials International*, 2014, **24**, 191.
- 50 M. V. Naseh, A. A. Khodadadi, Y. Mortazavi, F. Pourfayaz, O. Alizadeh, M. Maghrebi, *Carbon*, 2010, **48**, 1369.

- 51 R. S. Kalubarme, Y.H. Kim and C.J. Park. *Nanotechnology*, 2013, **24**, 365401.
- 52 M. Kim, Y. Hwang, K. Min, J. Kim. *Electrochimica Acta*. 2013, **113**, 322.
- 53 Y. Gao, L. Li, Y. Jin, Y. Wang, C. Yuan, Y. Wei, G. Chen, J. Ge, H. Lu, *Applied energy*, 2014, doi:10.1016/j.apenergy.2014.12.070.
- 54 L. Wang, X. Wang, B. Zou, X. Ma, Y. Qu, C. Rong, Y. Li, Y. Su, Z. Wang. *Bioresource Technology*, 2011, **102**, 8220.
- 55 G. Stephen Caravajal, D. E. Leyden, G. R. Quinting, and G. E. Maciel. *Anal. Chem.* 1988, **60**, 1776.
- 56 E.J.R Sudhölter, R. Huis, G. R. Hays, N.C.M Alma, 1985, **103**, 554.
- 57 G. Jakša, B. Štefane and J. Kovač, *Surf. Interface Anal.*, 2013, **45**, 1709
- 58 D. Kalderis, S. Bethanis, P. Paraskeva, E. Diamadopoulos, *Bioresource Technology*, 2008, **99**, 6809.
- 59 L. Wang, X. Wang, B. Zou, X. Ma, Y. Qu, C. Rong, Y. Li, Y. Su, Z. Wang *Bioresource Technology*, 2011, **102**, 8220.
- 60 H. Ismail, L. Mega, & HPS Abdul Khalil, *Polymer International*, 2001, **50**, 606.
- 61 A. Houshmand, W. M. Ashri Wan Daud. 978-0-9564263-4/5/\$25.00©2011 IEEE.
- 62 M. Selvi, S. Devaraju, K. Sethuraman and M. Alagar. *Polymer composite*, 2014, **35**, 2121.
- 63 T. Kosmidou, A.S. Vatalis, C.G. Delides, E. Logakis, P. Pissis and G.C. Papanicolaou, *eXPRESS Polymer Letters*, 2008, **2**, 364.
- 64 K.M. Jäger, D. H. McQueen. *Polymer*, 2001, **42**, 9575
- 65 L. Karásek, M. Sumita. *Journal of Materials Science*, 1996, **31**, 281.
- 66 S. Rastegar, Z. Ranjbar. *Progress in Organic Coatings*, 2008, **63**, 1.
- 67 F. E. Tantawy, K. Kamada, H. Ohnabe. *Materials Letters*, 2002, **57**, 242.
- 68 C. Han, A. Gu, G. Liang, L. Yuan. *Composites: Part A*, 2010, **41**, 1321.
- 69 X. Zhang, G. Liang, J. Chang, A. Gu, L. Yuan, W. Zhang. *Carbon*, 2012, **50**, 4995.
- 70 N. Nan, D. B. De Vallance, X. Xie and J. Wang. *Journal of composite materials*, 2015, doi: 10.1177/0021998315589770
- 71 R. Jan, M. Bilal Khan, Z. Mohammad Khan. *Materials Letters*, 2012, **70**, 155.
- 72 C.H. Ho, C.D. Liu, C.H. Hsieh, K.H. Hsieh, and S.N. Lee, *Synth. Met.*, 2008, **158**, 630.
- 73 U. Cano-Castillo and L. Rejon, *J. New Mat. Electrochem. Syst.*, 2001, **4**, 37.
- 74 M. Trihotri, U.K. Dwivedi, F. H. Khan, M.M. Malik, M.S. Qureshi. *Journal of Non-Crystalline Solids*, 2015, **421**, 1.
- 75 J. Xu, M. Wong, and C.P. Wong, *Electronic Components and Technology Conference*, 2004 **538**.
- 76 L. Zhu, *J. Phys. Chem. Lett.* 2014, **5**, 3677.
- 77 A. Dimiev, W. Lu, K. Zeller, B. Crowgey, L.C. Kempel, and J.M.Tour. *ACS Appl. Mater. Interfaces* 2011, **3**, 4657.
- 78 J. Chang, G. Liang, A. Gu, S. Cai, L. Yuan. *Carbon*, 2012, **50**, 689.
- 79 L. Cao, W. Zhang, X. Zhang, L. Yuan, G. Liang, and A. Gu. *Ind. Eng. Chem. Res.* 2014, **53**, 2661.

Exploring High k Dielectric Behavior of Bio-Carbon Reinforced Cyanate Ester Nanocomposites

Pichaimani Prabunathan^a, Krishnan Srinivasan^b, Arumugam Hariharan^b, and Muthukaruppan Alagar^{* a}

Table 1 Thermal Properties of Neat CE and FAC/CE nanocomposites

Sample	Tg (°C)	Temperature at characteristic weight loss (°C)		Char ratio at 900 °C (%)
		20%	60%	
Neat CE	234	243	270	6.0
1% FAC/CE	240	245	272	8.5
2% FAC/CE	245	248	276	9.5
3% FAC/CE	251	249	277	10.7
4% FAC/CE	259	251	278	11.2

Table 2 Elemental Compositions of neat CE and FAC/CE nanocomposites

Samples	Elements (wt %)				Total
	C	O	N	Si	
Neat CE matrix	68.01	26.33	5.66	-	100
2 % FAC/CE Nanocomposites	69.84	24.61	4.39	1.16	100
4 % FAC/CE Nanocomposites	74.52	20.50	2.53	2.45	100

Exploring High k Dielectric Behavior of Bio-Carbon Reinforced Cyanate Ester Nanocomposites

Pichaimani Prabunathan^a, Krishnan Srinivasan^b, Arumugam Hariharan^b, and Muthukaruppan Alagar*^a

^a*Polymer Composite Lab, Department of Chemical Engineering, Anna University, Chennai, 600 025, Tamilnadu, India.*

^b*Department of Chemistry, Anna University, Chennai 600 025, Tamilnadu, India.*

*E-mail : mkalagar@yahoo.com muthukaruppanalagar@gmail.com

Fax: +91 4422359164; Tel: +91 4422359164.

Graphical Abstract

Functionalized bio-carbon from rice husk is obtained and reinforced into cyanate ester matrix as embedded capacitor to achieve high k dielectric.

